



A High-Performance Mo₂C-ZrO₂ Anode Catalyst for Intermediate-Temperature Fuel Cells

Pilwon Heo,* Masahiro Nagao,* Mitsuru Sano, and Takashi Hibino**z

Graduate School of Environmental Studies, Nagoya University, Nagoya 464-8601, Japan

Anode performance of non-Pt catalysts for hydrogen oxidation was investigated in intermediate-temperature proton exchange membrane fuel cells. Molybdenum carbide (Mo₂C) showed the highest catalytic activity among the transition metal carbides tested. Furthermore, the catalytic activity of Mo₂C was significantly improved by the addition of ZrO₂ to the anode. Transmission electron microscopy and X-ray diffraction measurements revealed that Mo₂C was more highly dispersed in the Mo₂C-ZrO₂/C than in the Mo₂C/C, suggesting that the particle growth of Mo₂C was suppressed by the addition of ZrO₂. We also tested the performance of a fuel cell using Mo₂C-ZrO₂/C and Sn_{0.9}In_{0.1}P₂O₇ as the anode and electrolyte materials, respectively, between 150 and 300°C. At 250°C or higher, the Mo₂C-ZrO₂/C anode showed a cell performance comparable to that of the Pt/Canode. However, cell performance was strongly dependent on the operating temperature, reflecting that the catalytic activity of Mo₂C-ZrO₂ was greatly lowered by the decrease in operating temperature. Thus it was concluded that the Mo₂C-ZrO₂ catalyst is a promising alternative anode material to Pt, especially at intermediate temperatures.
© 2006 The Electrochemical Society. [DOI: 10.1149/1.2382268] All rights reserved.

Manuscript submitted July 11, 2006; revised manuscript received August 23, 2006. Available electronically November 16, 2006.

Recently, proton exchange membrane fuel cells (PEMFCs) have received increasing attention as next generation alternative power sources because of their high efficiencies and environmentally friendly characteristics. Proton-conducting fluoropolymers such as Nafion are commonly used as electrolyte membranes. However, these electrolytes present some challenges regarding technology and materials costs for the commercialization of PEMFCs.¹ Because protons attach themselves to water and diffuse as H₃O⁺ ions through the electrolyte, the operating temperature of PEMFCs is limited to the dehydration temperature of ~100°C, causing serious CO poisoning of the anode electrocatalysts. The electrolytes also need to be operated in highly humidified conditions, resulting in complicated water management. More importantly, the use of the expensive Pt catalyst is required to catalyze the electrode reactions at such low temperatures. These challenges would be overcome by using a proton conductor capable of operating above 100°C under low humidity or dry conditions. Thus, considerable efforts have been devoted to developing such proton conductors worldwide.²⁻⁷

We recently found that an anhydrous proton conductor, 10 mol% In³⁺-doped SnP₂O₇ (Sn_{0.9}In_{0.1}P₂O₇), showed high proton conductivities above 0.1 S cm⁻¹ between 150 and 350°C under unhumidified conditions.⁸⁻¹¹ The electromotive force values of a hydrogen concentration cell using this material were very near the theoretical values calculated by Nernst's equation, indicating that the ionic transport number was 0.97. A hydrogen/air fuel cell with a 0.35 mm thick Sn_{0.9}In_{0.1}P₂O₇ electrolyte could yield a high power density of 264 mW cm⁻² at 250°C. Furthermore, the fuel cell showed excellent tolerance toward 10% CO and good thermal stability under unhumidified conditions. However, there still remains the need to use Pt/C electrodes to achieve reasonable cell performance.

To date, low Pt loadings have been achieved by increasing the utilization of Pt and by alloying Pt with transition metals.^{12,13} However, there are no alternative electrodes showing as high a performance as Pt-based electrodes. Transition metal carbides such as Mo₂C and WC have been reported as potential catalysts for many chemical reactions because of their Pt-like behavior at elevated temperatures.¹⁴⁻²³ Mo₂C has also been investigated as an anode catalyst for PEMFCs,^{24,25} although its catalytic activity for electrochemical hydrogen oxidation is not high enough to meet the criteria for an alternative material. It is likely that the low catalytic activity of this material results from the low-temperature operation below 100°C.

In this paper, we report the anode performance of Mo₂C-based

catalysts toward hydrogen oxidation at intermediate temperatures between 150 and 300°C. The overpotential of Mo₂C was compared with those of other transition metal carbides and a Pt catalyst. Moreover, the catalytic activity of Mo₂C was improved by the addition of different metal oxides to the anode. Performance of a fuel cell with the optimized Mo₂C catalyst was evaluated in the temperature range from 150 to 300°C.

Experimental

Electrode preparation.—The Mo₂C/C anode was fabricated as follows. A MoCl₅ precursor was impregnated onto a carbon support (Black Pearls, Brunauer-Emmett-Teller surface area = 1500 m² g⁻¹). The impregnated sample was reduced in a 10 vol % H₂/Ar mixture at 500°C for 2 h and then carburized in a 20 vol % CH₄/H₂ mixture at 700°C for 3 h. Other transition metal carbides, MxC/C (M = W, Ni, Co), were prepared in a similar manner, although their carburization temperatures ranged from 700 to 1000°C, depending on the materials. The loading of all the carbides was 30 mg cm⁻². The Mo₂C/C anode was also modified by impregnating MoCl₅ along with various other metal chlorides or oxychlorides, such as ZrCl₂·8H₂O. Subsequent treatments were the same as those for Mo₂C. A Pt/C catalyst (30 wt % Pt/C, Tanaka Kikinokogyo) was used for comparison. The catalyst powder was mixed with 10% poly(vinylidene fluoride) (PVdF) binder in 1-methyl-2-pyrrolidinone (NMP) solvent using a mortar and pestle. However, because there is a possibility that PVdF melts above 200°C, the use of a more thermal-resistant binder would be necessary for practical applications. The mixture was coated on a carbon paper (Toray TGP-H-090). This sample was then dried for 1 h at 90°C, followed by 1 h at 130°C. A commercial Pt/C cathode (10 wt % Pt/C, 0.6 mg Pt cm⁻²) was purchased from E-TEK, Inc. The microstructure of the catalysts was analyzed using X-ray diffraction (XRD, Shimadzu XRD-600) and transmission electron microscopy (TEM, Hitachi H-800).

Electrolyte preparation.—Sn_{0.9}In_{0.1}P₂O₇ was prepared as described in our previous study.⁹ The corresponding oxides (SnO₂ and In₂O₃) were mixed with 85% H₃PO₄ and ion-exchanged water and then held at 300°C with stirring until the mixture turned into a paste with a high viscosity. After calcinating at 650°C for 2.5 h, the compound was ground with a mortar and pestle. The compound powders were pressed into a pellet 1.0 mm thick and 14.0 mm in diam under a pressure of 2 × 10³ kg cm⁻².

Fuel cell tests.—The anode and cathode (area = 0.5 cm²) were attached on opposite sides of the Sn_{0.9}In_{0.1}P₂O₇ electrolyte. Two gas chambers were set up by placing a cell between two alumina tubes. Each chamber was sealed with an inorganic adhesive. The fuel and

* Electrochemical Society Student Member.

** Electrochemical Society Active Member.

^z E-mail: hibino@urban.env.nagoya-u.ac.jp

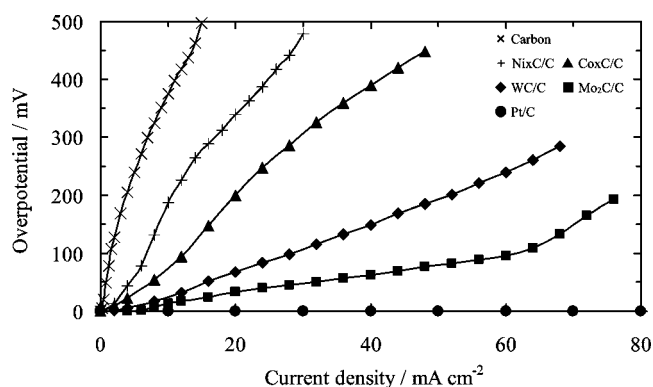


Figure 1. Anodic overpotentials of various carbon-supported transition metal carbide catalysts at 250°C. For comparison, the results obtained for Pt/C and carbon anodes are shown as well.

air chambers were supplied with unhumidified hydrogen and air, respectively, at a flow rate of 30 mL min⁻¹ between 150 and 300°C. The anodic overpotentials were analyzed by the current interruption method. In this case, a Pt reference electrode was attached on the surface of the side of the electrolyte. The voltage-current density curves were measured by the four-probe method between 150 and 300°C.

Results and Discussion

The anodic overpotentials of carbon-supported transition metal carbide anodes at 250°C are plotted in Fig. 1, including the results for Pt/C and carbon anodes. While the Pt/C anode showed negligibly small overpotentials, the carbon anode had significantly large overpotentials. The polarization resistances estimated from the slope of the potential vs the current density were 0.16 Ω cm² for Pt/C and 33.13 Ω cm² for carbon. Clearly, the catalyst-free hydrogen oxidation proceeded at a very slow rate even at 250°C. On the other hand, all of the metal carbide anodes showed lower overpotentials than that of the carbon anode. In particular, the Mo₂C/C anode exhibited the best performance among the carbides tested; the polarization resistance was 2.13 Ω cm². It is known that Mo₂C shows significant catalytic activities toward hydrogenation,¹⁸⁻²⁰ dehydrogenation,²¹ hydrodenitrogenation,²² and water gas shift reactions,²³ compared with the other metal carbides. It is also reported that Mo₂C has catalytic characteristics similar to those of Pt-group metals. Choi et al. have explained the unique catalytic activity of Mo₂C by the change in the electron density of the d-band of Mo upon its carburization.¹⁶ The introduction of C atoms into the Mo metal lattice leads to an increase in the lattice parameters, causing a contraction of the d-band and thus an enhanced d-electron density in the d-electron density levels of noble metals. However, Fig. 1 also shows that the performance of the Mo₂C/C anode was still considerably inferior to that of the Pt/C anode. In addition, there was an increase in the overpotential of the Mo₂C/C anode at high current densities, indicating a significant concentration overpotential based on mass transportation limitation. This may be due to an insufficient spill-over of hydrogen, causing a low hydrogen diffusion rate.

An attempt was made to improve the Mo₂C catalyst by the addition of various promoters to the catalyst. The chlorides or oxychlorides of Sn, Ce, W, and Zr were impregnated together with MoCl₅ onto a carbon support and then carburized at 700°C. As described below, the promoters were confirmed to be oxides rather than carbides after carburization. Figure 2 shows the anodic overpotentials of the unmodified and modified Mo₂C/C anodes at 250°C. All of the modified Mo₂C/C anodes, in particular Mo₂C-ZrO₂/C, showed considerably lower overpotentials compared to the unmodified Mo₂C/C anode. Moreover, there were no large increases in overpotential at high current densities. We chose ZrO₂, which showed the best performance, as a promoter for subsequent experiments.

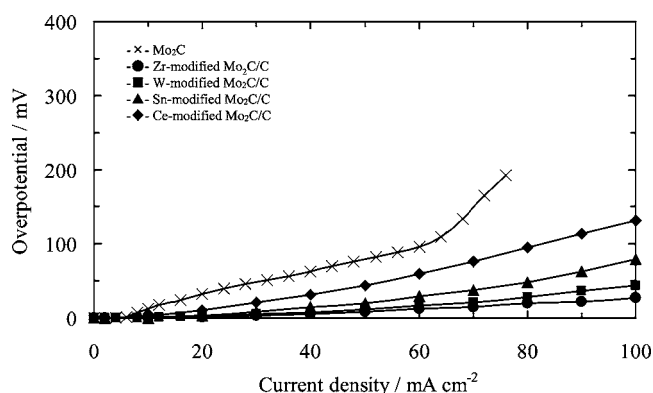


Figure 2. Anodic overpotentials of modified Mo₂C/C anodes at 250°C.

Figure 3 shows the anodic overpotentials of the modified Mo₂C/C anodes with different weight ratios of Mo₂C to ZrO₂ at 250°C. The overpotential decreased with increasing amount of ZrO₂ and reached a minimum at a weight ratio of Mo₂C:ZrO₂ of 1:0.2. The polarization resistance was 0.28 Ω cm², which was approximately one order of magnitude lower than that of the unmodified Mo₂C/C anode. On the other hand, the overpotential of the ZrO₂/C anode was much higher than that of the Mo₂C/C anode; the polarization resistance was 9.7 Ω cm². This result indicates that the effect of ZrO₂ shown in Fig. 3 is not attributable to the catalytic activity of ZrO₂ itself toward hydrogen oxidation.

To better understand the above effect of ZrO₂, the microstructure of the Mo₂C-ZrO₂/C catalyst was characterized by XRD and TEM measurements. Figure 4 shows XRD profiles of the Mo₂C/C and Mo₂C-ZrO₂/C catalysts. In the XRD profile of Mo₂C/C, all the diffraction peaks were identical to those reported for Mo₂C in the literature¹⁶ and no peaks of Mo metal and oxides were detected. The XRD profile of Mo₂C-ZrO₂/C revealed that the added Zr species was present as ZrO₂. In addition, the diffraction peaks of Mo₂C were not shifted by the addition of ZrO₂ to the catalyst, suggesting no incorporation of Zr into the crystalline lattice of Mo₂C. The Scherrer formula was used to estimate the particle size of Mo₂C. The estimated particle sizes were 28 and 13 nm for Mo₂C/C and Mo₂C-ZrO₂/C, respectively. A similar difference was observed in the particle size of Mo₂C, as revealed by transmission electron microscopy (TEM) measurements of the two catalysts. As shown in Fig. 5, the TEM images indicated that the particle sizes of Mo₂C were 16–34 nm and 10–16 nm for Mo₂C/C and Mo₂C-ZrO₂/C, respectively. These results indicate that the Mo₂C particles showed a higher dispersion with ZrO₂ than without ZrO₂. It is likely that excessive sintering of Mo₂C during carburization is inhibited in the

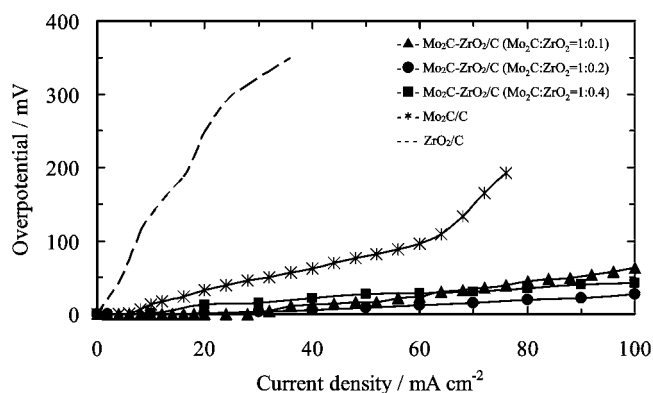


Figure 3. Anodic overpotentials of Mo₂C-ZrO₂/C anodes with different weight ratios of Mo₂C to ZrO₂ at 250°C.

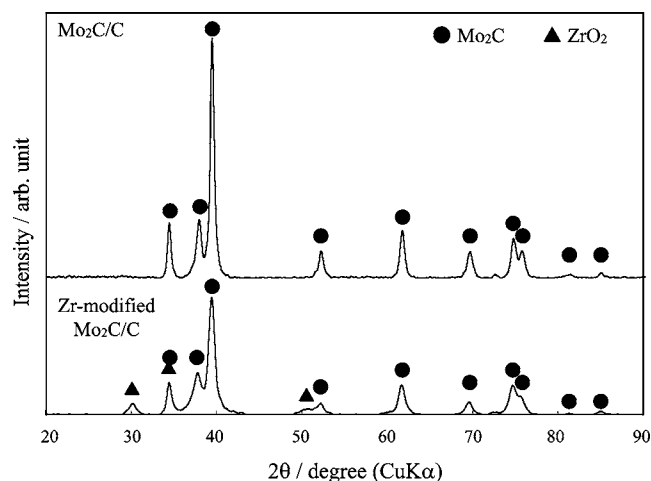


Figure 4. XRD profiles of $\text{Mo}_2\text{C}/\text{C}$ and $\text{Mo}_2\text{C}-\text{ZrO}_2/\text{C}$.

presence of ZrO_2 , resulting in the significantly improved catalytic activity of Mo_2C toward hydrogen oxidation. Naito et al. have reported that ZrO_2 was an effective support for Mo_2C in the reforming of CH_4 by CO_2 compared to other support materials such as SiO_2 , Al_2O_3 , ZrO_2 , TiO_2 , and CeO_2 .¹⁹ XPS analysis revealed a strong electronic interaction between Mo_2C and ZrO_2 in the $\text{Mo}_2\text{C}/\text{ZrO}_2$ catalyst. This interaction may be another reason for the promotive effect of ZrO_2 on Mo_2C .

Cell performance using the $\text{Mo}_2\text{C}-\text{ZrO}_2/\text{C}$ anode was evaluated at 250°C under unhumidified H_2/air fuel cell conditions. Figure 6 compares the cell performance using the $\text{Mo}_2\text{C}-\text{ZrO}_2/\text{C}$ anode with those using the $\text{Mo}_2\text{C}/\text{C}$, Pt/C , and carbon anodes at 250°C . The

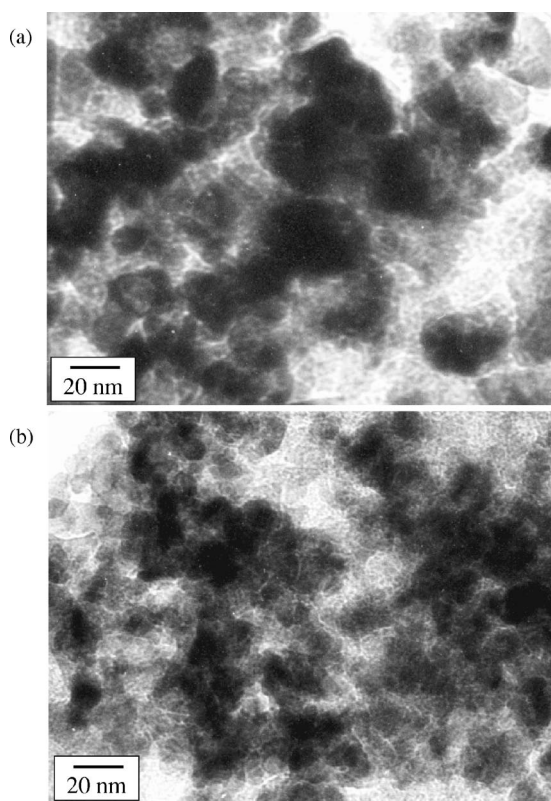


Figure 5. TEM images of $\text{Mo}_2\text{C}/\text{C}$ and $\text{Mo}_2\text{C}-\text{ZrO}_2/\text{C}$. The catalysts and carbons are shown as black and gray, respectively.

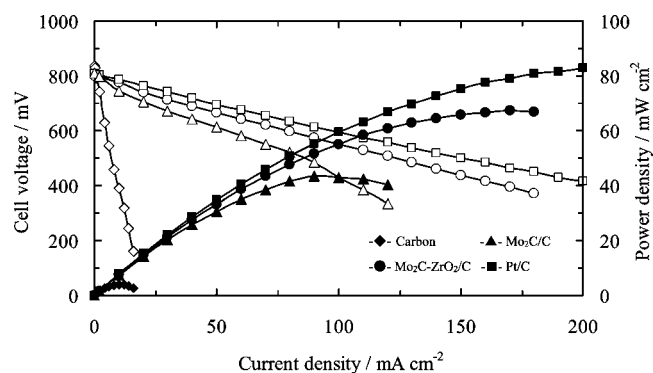


Figure 6. Cell voltage and power density vs current density of fuel cells with $\text{Mo}_2\text{C}/\text{C}$, $\text{Mo}_2\text{C}-\text{ZrO}_2/\text{C}$, Pt/C , and carbon anodes at 250°C . The thickness of the $\text{Sn}_{0.9}\text{In}_{0.1}\text{P}_2\text{O}_7$ electrolyte was 1 mm. The fuel and air chambers were supplied with unhumidified hydrogen and air, respectively, at a flow rate of 30 mL min^{-1} .

open-circuit voltages (OCVs) of all the fuel cells tested were between 0.80 and 0.85 V, which are lower than the theoretical value of ~ 1.1 V. The low OCVs are due to the physical leakage of gas through the electrolyte and partial electron-hole conduction in the electrolyte, as reported in previous studies.⁹ Note that while limiting current behavior was observed for the $\text{Mo}_2\text{C}/\text{C}$ anode at high current densities, no change in the current-voltage slope was observed for the $\text{Mo}_2\text{C}-\text{ZrO}_2/\text{C}$ anode, suggesting an enhanced hydrogen spill-over on the highly dispersed Mo_2C . More importantly, there is not a large difference in cell performance between the $\text{Mo}_2\text{C}-\text{ZrO}_2/\text{C}$ anode and the Pt/C anode; the power density was 67 mW cm^{-2} for $\text{Mo}_2\text{C}-\text{ZrO}_2/\text{C}$ and 84 mW cm^{-2} for Pt/C . This demonstrates that $\text{Mo}_2\text{C}-\text{ZrO}_2/\text{C}$ has a high potential as an anode catalyst for PEMFCs. However, this is not applicable to operation below 250°C . It can be seen from Fig. 7 that the cell performance with the $\text{Mo}_2\text{C}-\text{ZrO}_2/\text{C}$ anode was strongly dependent on the operating temperature; the peak power density reached 76 mW cm^{-2} at 300°C , but was significantly decreased at 200°C (35 mW cm^{-2}) and 150°C (28 mW cm^{-2}). The anodic overpotential measurements showed that the polarization resistance increased significantly with decreasing temperature, especially below 200°C ; the polarization resistance was $1.57\ \Omega\text{ cm}^2$ at 200°C and $2.15\ \Omega\text{ cm}^2$ at 150°C . Thus, it is concluded that the $\text{Mo}_2\text{C}-\text{ZrO}_2/\text{C}$ anode needs to be operated above 200°C for it to be an effective alternative to Pt-based anodes.

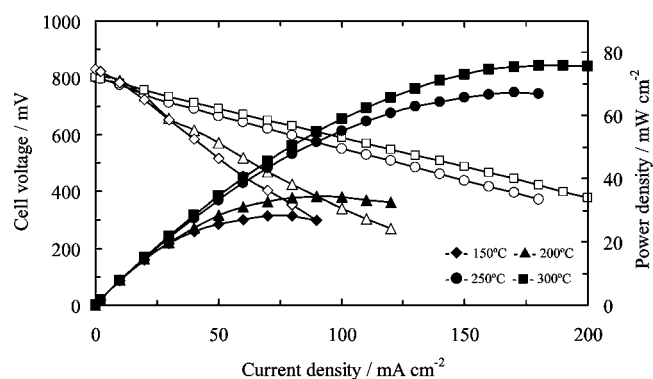


Figure 7. Cell voltage and power density vs current density of fuel cells with $\text{Mo}_2\text{C}-\text{ZrO}_2/\text{C}$ anode at different temperatures. The experimental conditions are the same as those shown in Fig. 6.

Conclusions

Anode performance of Mo₂C-based catalysts was studied at intermediate temperatures between 150 and 300°C. Although the Mo₂C catalyst showed the lowest polarization resistance at 250°C among all the transition metal carbide catalysts tested, its performance was still insufficient compared to that of a Pt catalyst. However, the addition of ZrO₂ to the catalyst allowed the Mo₂C to become highly dispersed on the carbon support, so that the catalytic activity could be improved to the level of the Pt catalyst. A fuel cell using the Mo₂C-ZrO₂/C and Sn_{0.9}In_{0.1}P₂O₇ as the anode and electrolyte, respectively, yielded a peak power density of 67 mW cm⁻² at 250°C, which was close to the peak power density of 84 mW cm⁻² obtained using a fuel cell with the Pt/C anode. This high performance of the Mo₂C-ZrO₂/C anode was achieved by intermediate-temperature operation above 200°C.

Nagoya University assisted in meeting the publication costs of this article.

References

1. B. C. H. Steele and A. Heinzl, *Nature (London)*, **414**, 345 (2001).
2. T. Uda, D. A. Boysen, and S. M. Haile, *Solid State Ionics*, **176**, 127 (2005).
3. S. M. Haile, D. A. Boysen, C. R. I. Chisholm, and R. B. Merle, *Nature (London)*, **410**, 910 (2001).
4. D. A. Boysen, T. Uda, C. R. I. Chisholm, and S. M. Haile, *Science*, **303**, 68 (2004).
5. W. Wiczorek, G. Zukowska, R. Borkowska, S. H. Chung, and S. Greenbaum, *Electrochim. Acta*, **46**, 1427 (2001).
6. A. Matsuda, T. Kanzaki, K. Tadanaga, M. Tatsumisago, and T. Minami, *Solid State Ionics*, **154-155**, 687 (2002).
7. J. D. Kim and I. Honma, *Electrochim. Acta*, **49**, 3179 (2004).
8. M. Nagao, T. Yoshii, T. Hibino, M. Sano, and A. Tomita, *Electrochem. Solid-State Lett.*, **9**, J1 (2006).
9. M. Nagao, A. Takeuchi, P. Heo, T. Hibino, M. Sano, and A. Tomita, *Electrochem. Solid-State Lett.*, **9**, A105 (2006).
10. P. Heo, H. Shibata, M. Nagao, T. Hibino, and M. Sano, *J. Electrochem. Soc.*, **153**, A897 (2006).
11. M. Nagao, T. Kamiya, P. Heo, A. Tomita, T. Hibino, and M. Sano, *J. Electrochem. Soc.*, **153**, A1604 (2006).
12. M. S. Wilson and S. Gottesfeld, *J. Appl. Electrochem.*, **22**, 1 (1992).
13. N. Cunningham, E. Irissou, M. Lefevre, M. C. Denis, D. Guay, and J. P. Dodelet, *Electrochem. Solid-State Lett.*, **6**, A125 (2003).
14. J. H. Sinfelt and D. J. C. Yates, *Nature (London), Phys. Sci.*, **229**, 27 (1971).
15. R. B. Levy and M. Boudart, *Science*, **181**, 547 (1973).
16. J. S. Choi, G. Bugli, and G. Djega-Mariadassou, *J. Catal.*, **193**, 238 (2000).
17. J. R. Kitchin, J. K. Nørskov, M. A. Barteau, and J. G. Chen, *Catal. Today*, **105**, 66 (2005).
18. D. C. LaMont and W. J. Thomson, *Chem. Eng. Sci.*, **60**, 3553 (2005).
19. S. Naito, M. Tsuji, and T. Miyao, *Catal. Today*, **77**, 161 (2002).
20. C. Sayag, M. Benkhaled, S. Suppan, J. Trawczynski, and G. Djega-Mariadassou, *Appl. Catal., A*, **275**, 15 (2004).
21. F. Solymosi, R. Nemeth, L. Ovari, and L. Egri, *J. Catal.*, **195**, 316 (2000).
22. S. Ramanathan and S. T. Oyama, *J. Phys. Chem.*, **99**, 16365 (1995).
23. J. Patt, D. J. Moon, C. Phillips, and L. Thomson, *Catal. Lett.*, **65**, 193 (2000).
24. E. C. Weigert, N. A. Smith, B. G. Willis, A. Amorelli, and J. G. Chen, *Electrochem. Solid-State Lett.*, **8**, A337 (2005).
25. T. Matsumoto, Y. Nagashima, T. Yamazaki, and J. Nakamura, *Electrochem. Solid-State Lett.*, **9**, A160 (2006).